ACS APPLIED MATERIALS & INTERFACES

www.acsami.org

Research Article

Solar Thermal Textiles for On-Body Radiative Energy Collection Inspired by Polar Animals

Wesley Viola, Peiyao Zhao, and Trisha L. Andrew*

Cite This: https://doi.org/10.1021/acsami.2c23075

Read Online

ACCESS | Metrics & More | Article Recommendations | Supporting Information

ABSTRACT: Humans use textiles to maintain thermal homeostasis amidst environmental extremes but known textiles have limited thermal windows. There is evidence that polar-dwelling animals have evolved a different mechanism of thermoregulation by using optical polymer materials to achieve an on-body "greenhouse" effect. Here, we design a bilayer textile to mimic these adaptations. Two ultralightweight fabrics with complementary optical functions, a polypropylene visible-transparent insulator and a nylon visible-absorber−infrared-reflector coated with a conjugated polymer, perform the same putative function as polar bear hair and skin, respectively. While retaining familiar textile qualities, these layers suppress dissipation of body heat and maximize radiative absorption of visible light. Under moderate illumination of 130 W/m^2, the textile achieves a heating effect of +10 °C relative to a typical cotton T-shirt which is 30% heavier. Current approaches to personal radiative heating are limited to absorber/reflector layer optimization alone and fail to reproduce the thermoregulation afforded by the absorber−transmitter structure of polar animal pelts. With increasing pressures to adapt to a rapidly changing climate, our work leverages optical polymers to bridge this gap and evolve the basic function of textiles.

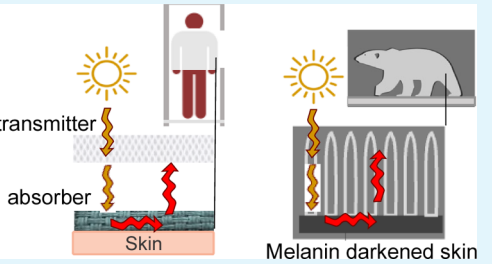

KEYWORDS: *chemical vapor deposition, solar thermal, textile coating, thermal management, extreme climate, infrared reflection, passive heating, energy saving*

1. INTRODUCTION

Wearable technology is advancing rapidly to bring a host of novel functionalities—health and environmental monitoring, motion tracking, and sleep evaluation—into everyday items. With a few exceptions, it is ironic that the first wearable—the textile—has not evolved in how it performs its original function: thermoregulation. Textiles have long been woven from fibers into thick structures that manage heat transfer by inhibiting thermal conduction and convection from the body to the environment while maintaining breathability. With increasing environmental and economic pressures to find more sustainable ways of living in a rapidly changing climate, it is necessary to leverage known materials and revisit the design of an old, basic technology—the textile.

In nature, organisms have met environmental challenges by manipulating light with optical materials for thermoregulation. Managing heat in a fundamentally different way than traditional textiles, specialized surfaces that selectively reflect, absorb, or transmit radiation across the visible and infrared (IR) spectrum allow certain animals to survive in severe conditions. This strategy is used by Saharan silver ants,[1] polar bears,[2] and moths.[3] There is convincing evidence that, under the extremely high solar insolation of the polar environment, certain cold-adapted animals use low optical density (lightly colored) insulating features to achieve a biological, on-body greenhouse effect.[4−6] Compared to darkly colored outer features, for example, the light-colored fur of the polar bear and harp seal transmits significantly more radiation toward the skin, trapping heat with solar utilization factors ranging from 10 to 50%.[6,7] Light-to-heat (photothermal) generation is enhanced by skin enrichment with melanin, an optically dense biopolymer comprised of conjugated units with a high refractive index and broadband light absorption.[8,9] Thermoregulating melanin surfaces are also used by species of moths, butterflies, and birds that have adapted to cold and sunny climates.[3,10] Such surfaces may also exhibit selective absorption in the visible and near-infrared (vis−NIR) spectrum, where photothermal heating takes place, and reflection over the infrared (IR), where objects spontaneously radiate heat according to Planck's law.[10] Solar collection supports thermal homeostasis by accessing a huge potential energy source with magnitudes exceeding 1000 W/m^2, i.e., up to 10 times the basal metabolic heat production of common endotherms.[11,12]

Radiative heating coatings of optical materials like MXenes, carbon nanotubes, and silver nanowires have been applied to

Received: December 28, 2022
Accepted: March 28, 2023

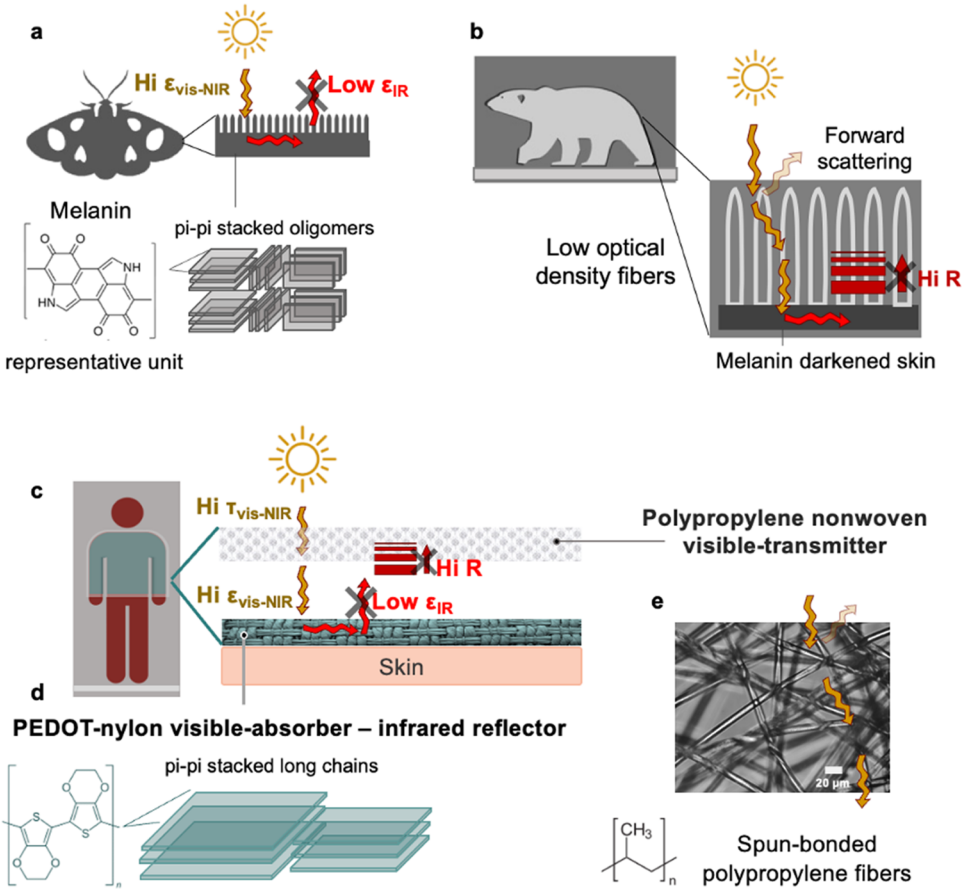

Figure 1. Designing a multilayer textile to mimic thermoregulation structures found in nature. (a, b) Animals that efficiently harvest solar thermal energy to reduce metabolic needs. (a) In the wings of certain moths and butterflies, melanin microstructures interact with light to control heat. The high optical density of melanin (representative structure shown) enables broadband light absorption and efficient light interference effects to suppress thermal emission. (b) Polar bear has similarly evolved melanin-enriched skin which may aid in photothermal capture. This effect may be enhanced by its unique hair-hollow and pigment-free fibers with a low optical density that forward-scatter light inward and inhibit thermal diffusion outward. (c) Our bilayer textile combines such light and heat control elements. (d) Bottom nylon fabric is vapor coated with PEDOT (structure shown), an optically dense organic conductor with high visible light absorption and low thermal emission. (e) Top fabric is made of spun-bonded polypropylene fibers (Agribon AG-19) and acts as a semitransparent insulator, transmitting 80% of visible light. A transmission optical micrograph shows the polypropylene fiber network. Scale bar 20 μm.

textiles to modulate radiative exchange via selective visible absorption and/or infrared reflection.[13−18] A crucial deficit distinguishing all such reported approaches from the adaptations of polar animals is the lack of an accompanying visible-transmitting outer layer that inhibits heat loss to the environment and, therefore, significantly amplifies the solar utilization factor. While the concept of visible-transmitting textiles has proven useful in agricultural and architectural applications—creating a local climate in a breathable, flexible format—its potential remains unexplored in direct, on-body heating.[19−21] Different in materials selection and purpose, the concept of infrared-transmitting, visible-opaque (ITVO) textiles is well reported on for personal radiative cooling.[22]

As an alternative to commonly reported visible absorber/infrared reflector inorganic or carbon nanomaterials listed above, certain polymers may be used for optically enabled thermoregulation.[9,23−25] Conjugated polymers are one such class of soft materials particularly suited for textile applications. Robust, skin-compatible coatings of such polymers on complex surfaces characteristic of fabrics are achievable with oxidative chemical vapor deposition.[26] Similar to melanin, polymers like poly(3,4-ethylenedioxythiophene) (PEDOT) exhibit high optical density with electromagnetic properties arising from $\pi-\pi$ stacked conjugated units.[27] While being lightweight and flexible, conjugated polymers are also often water-swellable and possess chemical structures that bear resemblance to those of the optically active biopolymer melanin described previously.[28]

In this paper, we create a lightweight textile platform for on-body light and heat management by taking inspiration from natural structures found in the polar environment. Our approach is to pair a visible-transmitting textile outer layer with a visible-absorbing−infrared-reflecting base layer to mimic the translucent fur and melanized skin, respectively, of the cold-adapted polar bear. Previous reports of wearable polar bear fur mimics fail to reproduce this transmitter−absorber structure (Figure S1). Using this design, we demonstrate that an all-polymer garment can achieve extreme thermoregulation efficiency by passive photothermal heating in moderate light conditions. The transmissivity and absorptivity of the two fabric layers is characterized across the visible and infrared spectrums and compared with common fabrics in the context of solar collection potential. A climate-controlled chamber with a skin and solar simulator is then used to evaluate the heating performance relative to common garments. Exposed to a

https://doi.org/10.1021/acsami.2c23075
ACS Appl. Mater. Interfaces XXXX, XXX, XXX−XXX

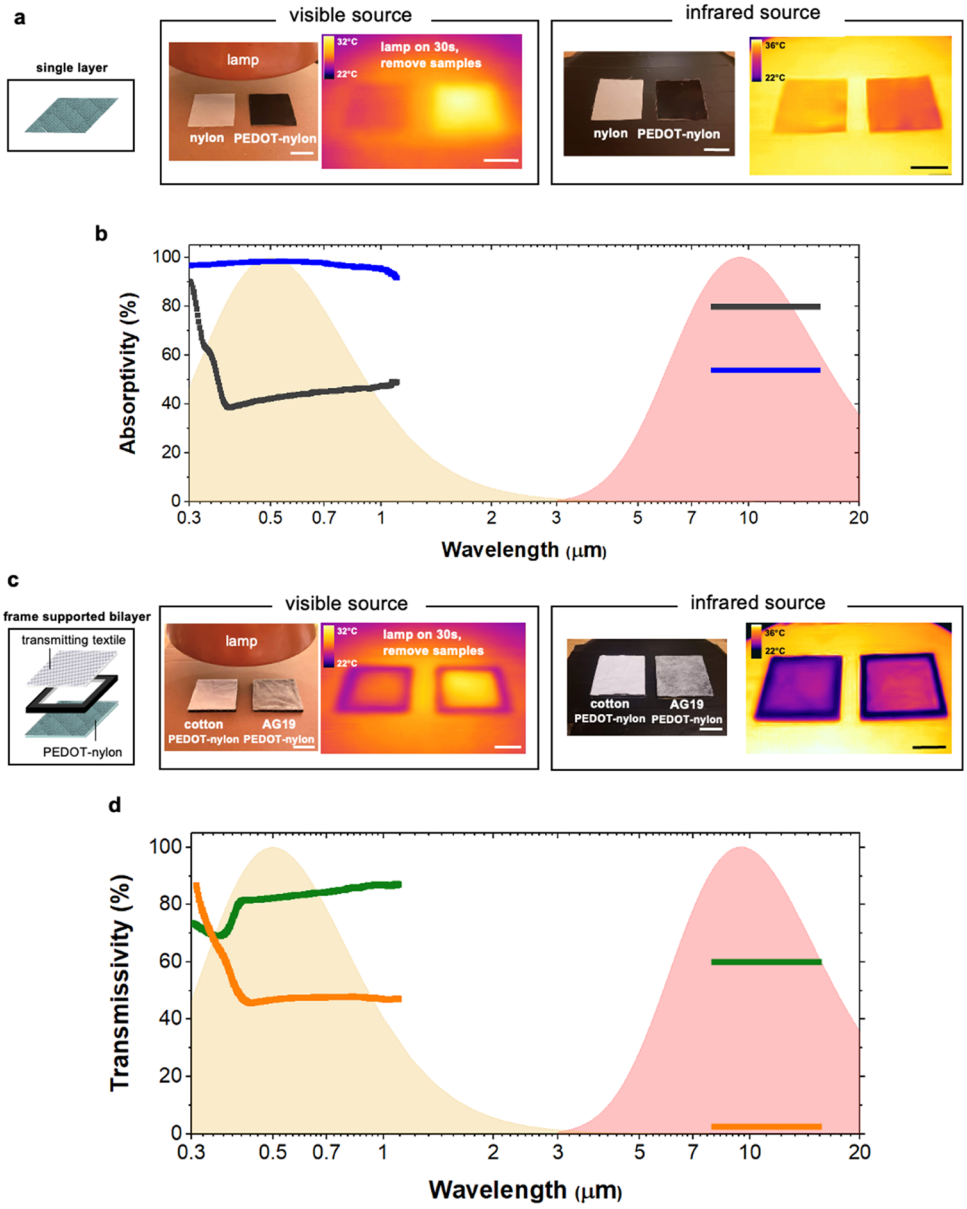

Figure 2. Characterizing the optical properties of PEDOT-nylon and AG-19 fabrics. (a) Photographs and infrared (IR) images of uncoated and coated nylon fabric interacting with a visible light source (lamp) and an IR source (heated copper block). Scale bars 2.5 cm. (b) Absorptivity of PEDOT-coated nylon (blue) relative to uncoated (black) compared against the blackbody spectra of the sun (5504 °C) and human body (33 °C). Data collected for the range 8−14 μm are averages. (c) Characterizing PEDOT-nylon bilayer textiles (structure shown) with a cotton jersey top layer and an AG-19 top layer. (d) Transmissivity of cotton (orange) and AG-19 (green) fabrics.

moderate light intensity of 130 W/m^2 (ca. 0.1 sun), this thermal textile has a temperature rating that extends 9.9 °C lower than a typical cotton fabric (4.2 °C/~40 °F versus 14.1 °C/~60 °F, respectively) while weighing 30% less. A steady-state heat transfer model that considers solar absorbance and infrared absorptivity is developed to understand the performance limits of a spectrally optimized absorber layer.

2. RESULTS

2.1. Biomimetic System Design and Materials Selection. Traditionally, textiles have been made from a limited material set. Natural or synthetic fibers are spun and woven into thick fabrics that inhibit heat diffusion between the body and the environment. Perhaps due to the lack of suitable materials, traditional textile design has largely overlooked the management of radiative heat (i.e., energy carried by light). Recently, this has begun to change with, for example, the development of radiative heating textiles enabled by reflective metallic coatings[29] and radiative cooling textiles enabled by infrared-transparent, visible-opaque polyethylene fabrics.[22] A performance gap still exists for more efficient personal heating in a comfortable, familiar textile format. One way forward is to limit dissipation of radiant body heat outward while optimizing absorption of ambient radiant energy inward. The power density of sunlight, for example, is sufficient (100−1000 W/m^2) to supplement typical metabolic heat production (~70 to 120 W/m^2). It is therefore unsurprising to see both directions of radiative energy management in adaptations of polar animals.

https://doi.org/10.1021/acsami.2c23075
ACS Appl. Mater. Interfaces XXXX, XXX, XXX−XXX

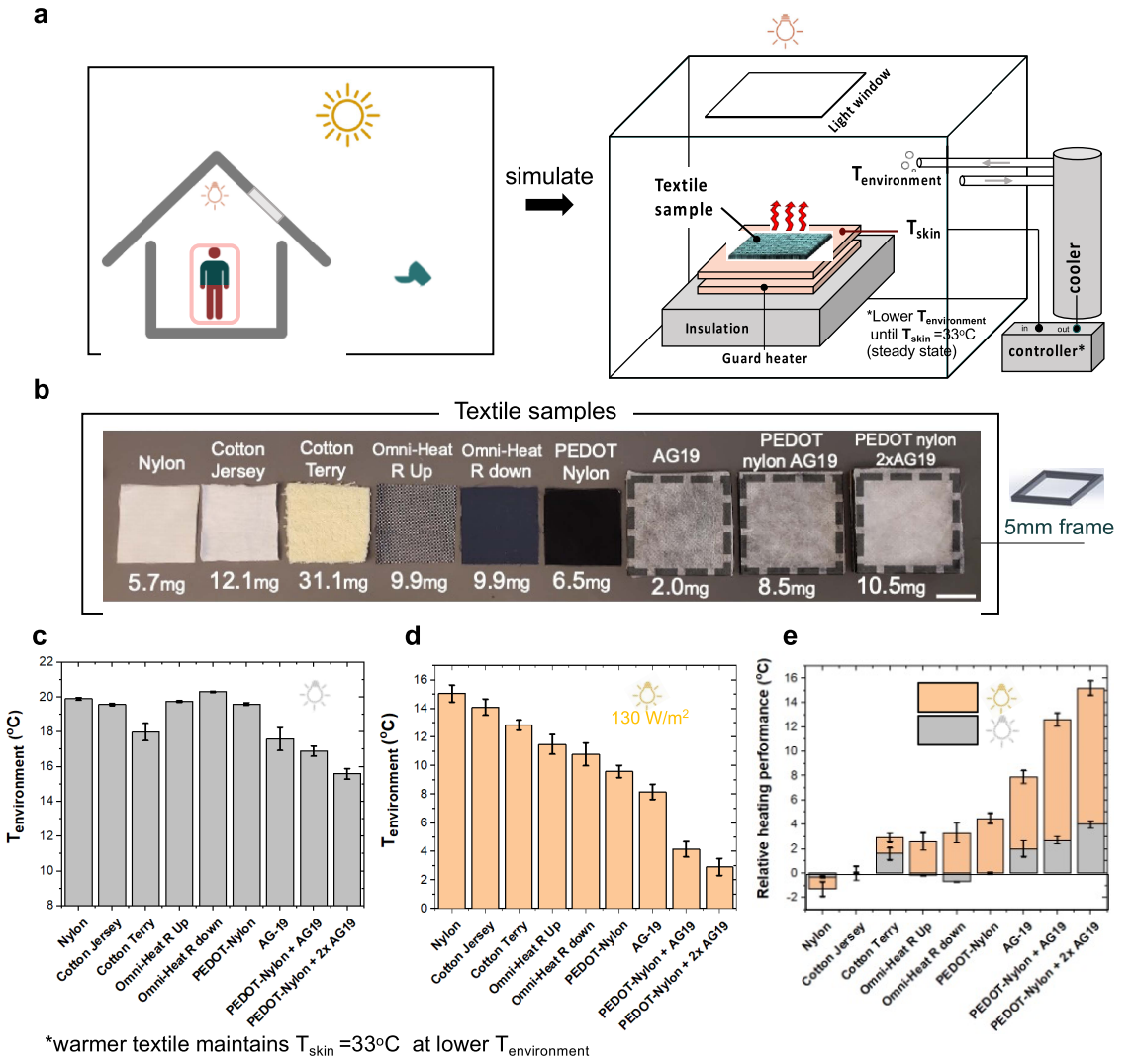

Figure 3. Characterizing the thermoregulation of traditional and novel textiles. (a) Textiles control heat transfer between the body and environment but are not currently optimized to collect indoor or outdoor light as heat. A chamber is used to simulate such heat transfer and evaluate the low temperature ratings of textile samples in varying ambient light conditions. The skin surface is simulated by a heater with a constant output (Q_{gen}). To characterize a sample, a microcontroller monitors the skin temperature (T_{skin}) and finds the lowest environmental temperature ($T_{environment}$) that is thermally comfortable (T_{skin} = 33 °C). Warmer textiles have lower environmental temperature ratings. Ambient light exposure is varied. (b) Textile samples characterized. Fabric weights (mg/cm^2) are shown. Scale bar 2.5 cm. Temperature ratings of textiles exposed to (c) dark and (d) light (130 W/m^2) conditions. (e) Relative heating performance. Positive values indicate an extension of the textile temperature rating relative to a typical cotton jersey (T-shirt) fabric.

Two natural structures inspire the design of our solar thermal textile. The first is a type of structural coloration in some species of cold-adapted moths and butterflies that enables selective absorption of visible−NIR light and suppression of thermal (IR) emission (Figure 1a).[3,10] In this case, melanin is the optically active material. With an electron-dense $\pi-\pi$ stacked structure, melanin behaves as a disordered (having more amorphous than crystalline sites) organic semiconductor and has a significantly higher refractive index than most biopolymers.[8,9] A variety of donor−acceptor units enable broadband light absorption, while a high optical density enables light interference effects (IR reflection) in melanin-enriched wing coatings.[10]

The second source of inspiration is the pelt of the polar bear which, key to the animal's survival in the extreme cold, simultaneously provides high thermal resistance (R) and high solar utilization (Figure 1b). The dual function arises from a specific material set and optical structure. Lacking melanin pigment, hollow hair fibers have a low optical density and efficiently forward-scatter light, permitting photothermal capture at the melanized skin while inhibiting heat loss to the environment.[2,6,11,19,30] The essential optical structure of the pelt—a transmitter−insulator (transparent hair) stacked above an absorber (darkened skin)—efficiently harvests solar thermal energy to support thermoregulation in the extreme cold. While several groups have reported personal heating materials nominally mimicking polar bear fur, none have demonstrated this crucial optical structure nor a transmitting insulator fabric.[31−33] More accurate polar bear inspired textiles and structures have been reported for building-level solar collectors,[19,34,35] but here we analyze the energetic significance of direct radiative capture at the body−environment interface and show the high thermoregulation efficiency of a wearable solar thermal textile.

https://doi.org/10.1021/acsami.2c23075
ACS Appl. Mater. Interfaces XXXX, XXX, XXX−XXX

To mimic such adaptations, we engineered a bilayer textile using optical polymer materials (Figure 1c). The bottom layer is a nylon fabric robustly vapor coated with the conjugated polymer PEDOT, enabling selective absorption of visible light and suppression of IR emission. In structure and function, the soft material PEDOT resembles melanin. This $\pi-\pi$ stacked electronic polymer interacts strongly with light due to high free-electron density associated with long conjugated chains.[36] While PEDOT is an organic *conductor*, it shares the same broadband vis−NIR light absorption of melanin due to plasmon (surface electron) resonance near 1000 nm with a high optical density κ.[27] At longer wavelengths into the IR, PEDOT is a reflector (a weak emitter). Like the melanin-enriched microstructure of moth wings, a PEDOT coating can therefore be used to efficiently manage radiative heat transfer between the body and the environment.

Photothermal heat generated at the PEDOT-nylon absorber is further trapped by the top layer, a semitransparent fabric mimicking the light-colored fur of polar animals. This lightweight fabric (Agribon AG-19)[20] is made of low optical density polypropylene fibers that forward-scatter visible light with about 80% transmission and more weakly transmit IR light with about 60% transmission. By confining solar thermal heat as both a diffusion and IR radiation barrier, AG-19 essentially acts like a breathable "greenhouse" material. Indeed, AG-19 is used in the agricultural industry for this purpose. Individual fibers are visualized in an optical transmission micrograph in Figure 1e. Fiber diameter is in the range of 9−10 μm, comparable to IR wavelengths and thus capable of Mie scattering to trap IR radiation.[37] As with polyethylene and other polyolefins, polypropylene is an attractive material for textiles for its potential sustainability, durability, and ultralightweight.[22] Along with the spectrally selective PEDOT-nylon fabric, the fabric transmitter layer operates differently than traditional textiles and has the potential to provide more efficient thermoregulation.

2.2. Optical and Thermoregulation Characterization of Absorber and Transmitter Fabrics. A 1-μm thick coating of PEDOT onto nylon fabric dramatically changes the surface optical properties due to the high optical density of PEDOT. Figure 2a visualizes this change in photographs and thermal images. Under a commercial lightbulb, the coated fabric absorbs more photothermal energy relative to the uncoated nylon and transfers this heat to the underlying surface. Over an IR source (heated copper plate), the coated fabric emits less thermal energy (appears "colder") than the high absorptivity (emissivity) surface of the uncoated nylon. These effects are quantified in Figure 2b, where absorptivity of the coated fabric (blue) and uncoated (black) is plotted against wavelength. The uncoated nylon fabric shows a behavior typical of traditional textiles: low absorptivity in the visible and high absorptivity in the IR. With a PEDOT coating, this optical behavior is reversed, and the fabric behaves more like an ideal photothermal absorber. PEDOT coatings of 1 μm thickness were used for fabric coatings to maximize the NIR (>800 nm) absorption of the samples (Figure S2). The visible−NIR absorbance of PEDOT is in the range of absorbance values reported for some carbon nanomaterials used in personal thermoregulation while IR reflectance of PEDOT is significantly higher relative to carbon nanotubes.[31,33]

The photothermal heat trapping of the lightly colored visible-transmitting textile is also visually characterized in an absorber−transmitter bilayer structure supported by a 5 mm thick frame (Figure 2c). As compared to a cotton−PEDOT-nylon bilayer, the AG-19−PEDOT-nylon bilayer traps significantly more thermal energy under a visible light source. Over the infrared source, more thermal emittance is observed through the AG-19 layer. Figure 2d presents the transmissivity of the cotton (orange) and AG-19 (green) fabrics: the high solar thermal efficiency of the AG-19 fabric is owed to high visible light transmission (80%) relative to the more opaque cotton (55%). This optical distinction may be attributed not just to fiber material differences between the cotton and AG-19 but also to the low packing density of the AG-19.

With optically active fabrics, we next evaluate the thermoregulating performance of a set of traditional and novel fabrics. A simple way to conceptualize this task is by considering the lowest temperature rating for which a certain textile can maintain the wearer's thermal comfort. Warmer textiles are needed for colder environments (Figure 3a). More specifically, a textile should limit the loss of body heat (~75 W/m^2 for an average adult at rest) to the environment so that a comfortable skin temperature (~33 °C) is maintained at steady state.[38] Excluding factors like wind chill and humidity, this situation is simulated in a chamber depicted in Figure 3b. For a given textile sample, the temperature of a skin heater with a constant output is monitored by a controller that lowers the environmental temperature until thermal comfort (T_{skin} = 33 °C) is reached at steady state. A similar chamber design was previously used to evaluate passive heating solutions,[29] except here a window allows for environmental light (radiative energy) input to the textile−skin system.

Uncoated and PEDOT-coated nylon were tested, as well as a range of traditional and nontraditional textile comparators of varying weights, as shown in Figure 3c. A cotton jersey sample represents typical T-shirt material, while cotton terry is typical of heavier, warmer garments like a sweatshirt. The other optically active textiles include commercial Omni-Heat and spun-bonded polypropylene (AG-19). The Omni-Heat fabric is tested with the reflective face up (R up) and down (R down). The AG-19 is held by a 5 mm thick plastic frame for consistency across measurements. The low temperature ratings of the textiles were measured in the environmental chamber and results for dark conditions are shown in Figure 3c. The low emissivity fabrics—PEDOT-nylon and Omni-Heat (R up)—perform similarly to the cotton jersey fabric as has been previously demonstrated.[29] The thicker cotton terry and AG-19 fabrics offer more insulation and have lower environmental temperature ratings in the range of 18 °C.

Under moderate illumination of 130 W/m^2, the performance of the textile samples varies more widely. While the PEDOT-nylon and Omni-Heat (R up) fabrics perform similarly in dark conditions due to comparable thermal emissivity values, the PEDOT-nylon has a greater visible absorbance and so performs significantly better under illumination (9.6 °C versus 11.5 °C). Compared with PEDOT fabrics, other metal-coated textiles may show poor solar thermal heating due to the higher resonant frequencies (in the UV−visible range) of commonly used metals like aluminum and silver.[39] Individually, AG-19 also performs well (8.2 °C) but when stacked in the absorber−transmitter structure, the complementary optical functions of the PEDOT-nylon and AG-19 yield a more dramatic heating effect. The bilayer textile has a temperature rating that extends 10 °C lower than the cotton jersey fabric (4.2 °C/~40 °F versus 14.1 °C/~60 °F) while weighing 30% less. With an

https://doi.org/10.1021/acsami.2c23075
ACS Appl. Mater. Interfaces XXXX, XXX, XXX−XXX

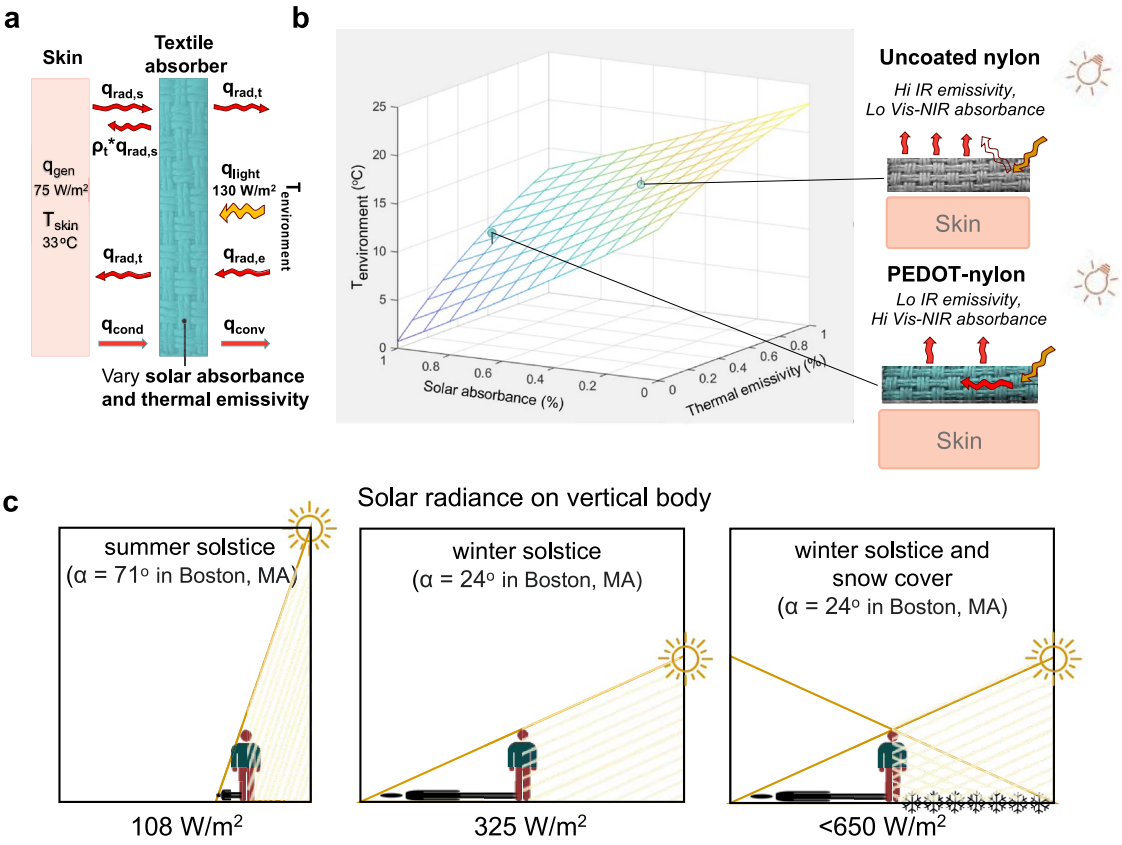

Figure 4. Modeling the impact of optical properties on textile thermoregulation for a moderate light intensity of 130 W/m^2. (a) Schematic of the steady-state heat transfer model for a single-layer textile. $T_{environment}$ is calculated as a function of textile spectral selectivity given the thermal comfort condition (T_{skin} = 33 °C). (b) Results of the simulation. Textile thermoregulation is optimized at high solar absorbance and low thermal emissivity. Two experimental points (uncoated and PEDOT-coated nylon) are shown. (c) Approximation of solar radiance on a vertical body at high latitude (Boston, MA). The coldest season may correspond with the maximum radiance due to reduced solar elevation; snow cover (albedo >90%) as much as doubles light exposure. The human body is taken as a vertical cylinder and incident radiance, illuminating half of the body area, is divided by the total surface area.

additional layer of AG-19, the performance improves more modestly (extending to 2.9 °C), suggesting that the sacrifice of solar utilization (light transmission) for thermal insulation becomes less favorable to thermoregulation.

Taking the temperature rating of the cotton jersey fabric as a baseline for the other measurements allows comparison of textile performance in both light and dark conditions (Figure 3e). While the thick, insulating cotton terry fabric shows strong performance in dark conditions (+1.6 °C relative to cotton jersey), it has relatively weak performance in light conditions (+1.3 °C). This is representative of traditional textiles—thick, opaque insulation that limits heat dissipation outward also necessarily limits photothermal heat transfer inward. On the other hand, the bilayer textile excels in both dark (+2.7 °C) and light (+9.9 °C) conditions due to the insulating yet light-transmitting AG-19 layer.

Other wearable photothermal mimics comprise outward-facing darkly colored surfaces,[31−33] which may explain the reduced solar heating effect (relative to cotton T-shirt, +5.5 °C versus +9.9 °C) of one such report (Figure S1). We confirm the importance of optical structure by reversing our absorber−transmitter stack, i.e., facing the dark-colored PEDOT surface outward, which significantly reduces relative performance (+7.1 °C versus +9.9 °C) (Figure S3). This agrees with counterintuitive observations that darker-colored pelt features, due to inhibited light transmission, may achieve less solar utilization than light-colored pelts.[6,7,11]

2.3. Modeling Textile Thermoregulation under Illumination. While previous work in radiative heating textiles has studied the impact of IR surface properties,[29] here we study the combined impact of IR and visible optical properties on personal heating under moderate light intensity. As a simple case, we focus on an absorber-only system which, due to the broad IR and visible transparency of the AG-19 transmitter layer, might behave similarly to the absorber−transmitter system as the absorber optics are varied (Figures S4 and S5). Our steady-state heat transfer model (Supporting Note 1) of the skin−textile system includes incident radiation (130 W/m^2) and a natural convection coefficient that varies with the skin−environment temperature difference (Figure 4a). The results of the simulation are shown in Figure 4b and experimental data points of uncoated and PEDOT-coated nylon are overlaid. The performance of the radiative heated textile is optimized at maximum solar absorbance and minimum thermal emissivity, and we note that the PEDOT coating brings the nylon fabric closer to this target. At 130 W/m^2, the dependence of environmental temperature on solar absorbance is roughly comparable to that of thermal emissivity; however, at greater radiance (325 W/m^2), solar absorbance becomes the dominant contributor (Figure S6).

https://doi.org/10.1021/acsami.2c23075
ACS Appl. Mater. Interfaces XXXX, XXX, XXX−XXX

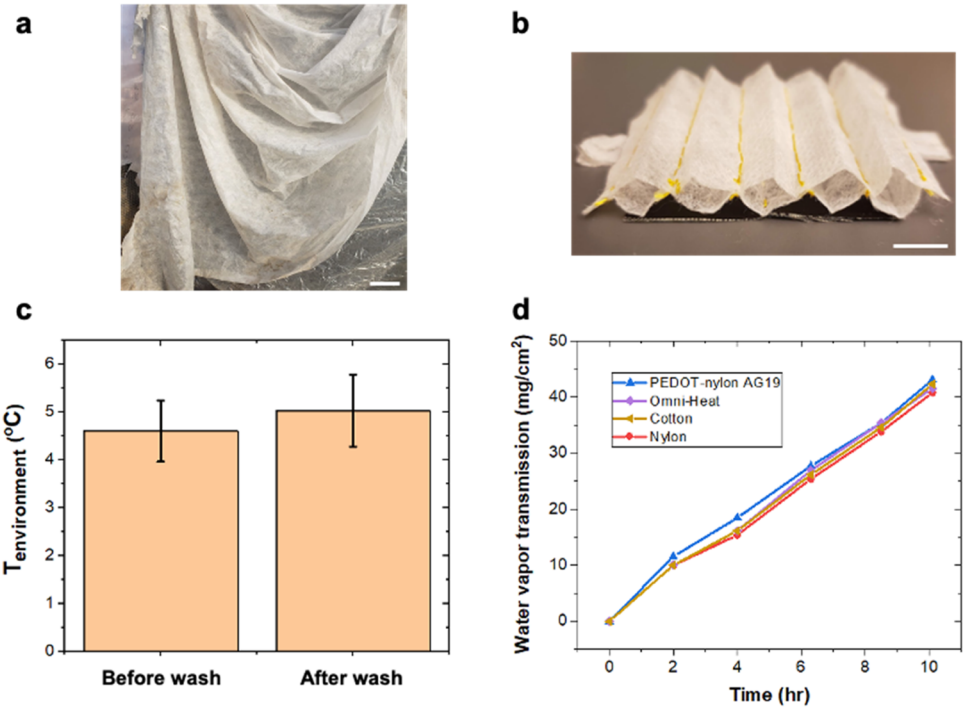

Figure 5. Practical characteristics of the solar thermal textile. (a) Nonwoven AG-19 fabric exhibits drapeability. (b) Two layers of AG-19 are sewn together and ironed to make insulating baffles. The PEDOT-nylon layer is then sewn to the bottom. (c) Textile thermoregulation characterization across three washing cycles. (d) Breathability characterization shows similar water vapor transmission across the textiles tested.

To understand realistic sunlight utilization, the human body is approximated as a vertical cylinder and normal incident radiance per total surface area (typically 1.8 m^2) is calculated across the year assuming half of the body is illuminated.[40] For solar-powered personal heating, a convenient coincidence is that the coldest season may correspond with the maximum solar radiance on a vertical body due to the reduced solar elevation. In Boston, MA, for example, the calculated on-body radiance of direct sunlight increases from about 108 W/m^2 at the summer solstice to about 325 W/m^2 at the winter solstice. The presence of snow fields can also dramatically increase overall solar insolation values, as is the case in polar environments, which as much as doubles the direct solar contribution.[5] With a combined body-surface irradiance of 650 W/m^2, the available wintertime solar thermal power at high latitudes may therefore be nearly 10 times larger than the body heat generated by a moderately active adult (70−120 W/m^2).[38] The bulky, opaque nature of winter outerwear assures low utilization of this power source, as the weak solar heating of the thick cotton terry fabric demonstrated above suggests. On the other hand, the bilayer textile described here utilizes environmental light to provide remarkable heating for its weight. Exposed to the calculated wintertime radiance of 650 W/m^2, the textile supports thermal homeostasis as low as −28 °C (Figure S7), approaching the temperature extremes of the polar environment. Indoors, a light capturing textile can support the development of passive solar architectures[41] as personal heating and design elements, as well as be powered by existing indoor light fixtures capable of the lower radiance levels modeled here.[42]

2.4. Wearability Characterization. Everyday clothing is expected to be comfortable, breathable, and washable. The optically active textiles presented herein were also evaluated for these functions. Despite being nonwoven, the AG-19 transmitter fabric has many familiar textile qualities that make it suitable for garments and apparel, upholstery, and decor. The nonwoven fabric may be draped (Figure 5a), sewn, and ironed without damage. Advancing from the frame-supported textile presented earlier, we next demonstrate the use of such materials in a self-supported garment made by sewing two layers of AG-19 and ironing pleats to form insulating baffles. PEDOT-nylon is then sewn to the bottom to complete the solar thermal textile (Figure 5b). This textile performs similarly to the previously characterized bilayer structure and, importantly, is stable after three washing cycles using common laundry detergent and after 2 total hours of light exposure (130 W/m^2) (Figure 5c). Optical microscopy of the PEDOT coating across washings shows a small change in color and no damage to the mechanical stability of the films (Figure S8). A water vapor transmission test across an AG-19/PEDOT-nylon stack reveals that this bilayer is as breathable as other common fabrics used in the study (Figure 5d). This is unsurprising given the diffuse open mesh of the AG-19 fabric, designed to be breathable, and the hydrophilic nature of PEDOT.[28]

3. CONCLUSIONS

Here, we leverage optical polymer materials to design a radiative heating textile as a mimic of the absorber−transmitter structure of the polar bear skin and fur and are the first to demonstrate the dramatic personal heating effect this structure has when worn on the body. While retaining familiar textile qualities, the bilayer design suppresses radiative dissipation of body heat and maximizes radiative absorption of visible−NIR light. Due to a faithful imitation of the light collecting structure and function of polar bear pelt, the garment achieves a significantly greater personal heating performance than other nominal mimics which lack visible-transmitter fabrics.[31−33] Under moderate illumination of 130 W/m^2 (ca. 0.1 sun), this

https://doi.org/10.1021/acsami.2c23075
ACS Appl. Mater. Interfaces XXXX, XXX, XXX−XXX

textile maintains the wearer's thermal comfort down to 4.2 °C—an additional heating effect of 10 °C relative to a typical cotton T-shirt that is 30% heavier. Under a radiance of 650 W/m^2, representative of wintertime sunlight at high latitudes, the garment supports thermal homeostasis in still air as cold as −28 °C.

Using similar design methods, it is also possible to adapt our strategy to radiative cooling and access a reflector−emitter structure like that found on the Saharan silver ant.[1] By rejecting solar heat and dissipating thermal heat through the atmospheric window, such a structure may allow adaptive living in extremely hot conditions. The material properties and vapor deposition of PEDOT can enable different kinds of optical control beyond the photothermal effect shown here. When used with specific surface geometries, the plasmon-coupled light interactions of PEDOT can also be directed to produce the high reflectivity needed for daytime radiative cooling.[43−46] The oxidative vapor deposition process used in this work is uniquely suited for such optical engineering purposes. Electronic polymer coatings of precise thickness can be conformally deposited over complex surface arrays which may, like the faceted triangular hairs that endow the silver ant with its optical thermoregulation, possess features ranging in size from submicron to micron.[47] The second adaption of our strategy involves designing a transparent thermal emitter layer. While the polypropylene fibers here primarily serve to transmit visible light, Mie scattering theory informs optical tuning toward high IR emittance by adjusting fiber size and geometry to achieve dielectric resonance at IR frequencies.[48]

The solar thermal textile presented here is a flexible, lightweight platform for collecting radiative energy. Indoors, this technology can enable efficient thermoregulation by local, low-power lighting (i.e., LEDs) as well as support the design of passive solar architectures. Outdoors, a lightweight solar textile design will improve winterwear and enable passively heated shelters for adaptive living in harsher climates. As the energy and environmental crises progress, reinventing textiles with polymer-enabled light and heat control will prove increasingly useful.

4. EXPERIMENTAL DETAILS

4.1. PEDOT Film Deposition. Films of PEDOT-Cl were deposited onto ripstop nylon using a custom-built reactor and the process described in previous reports.[26] Briefly, 3,4-ethylenedioxythiophene (EDOT) (95%, TCI America) was reacted with iron(III) chloride ($FeCl_3$) (97%, Sigma-Aldrich) in the vapor phase at low pressures maintained at ∼750 mTorr. EDOT was evaporated at 95 °C and delivered into the chamber via a needle valve (Swagelok SS-4JB) that was typically opened a quarter turn. The volume of EDOT in the glass bulb was monitored over the course of the deposition to ensure a monomer flow rate of 5−10 sccm. $FeCl_3$ was sublimed by heating to >205 °C in a Luxel RADAK II furnace. The substrate stage was heated to 150 °C over the course of the deposition. Real-time film growth rate was monitored by a quartz crystal microbalance (QCM) located inside the chamber. Due to the different positioning of the QCM relative to the sample stage, a correction factor is needed to account for film growth rate variations. By measuring actual film thickness postdeposition using a Dektak profilometer, a tooling factor of 0.24 was determined. Film growth rate was kept at 2 nm/s. After the desired film thickness was reached, the sample stage was allowed to cool below 60 °C under vacuum. To remove residual iron salts and oligomers, samples were immediately rinsed with dilute acid (0.5 M HCl) for 30 min, followed by a methanol rinse.

4.2. Textiles. Agribon AG-19 (140 μm thickness measured with calipers) was purchased from Johnny's Selected Seeds. Ripstop nylon (60 μm), cotton terry (1000 μm), and cotton jersey (310 μm) were purchased from Joann's Fabrics. Samples were cut to 5 × 5 cm^2 dimensions. Agribon samples were cut to 6x6cm dimensions and supported by a 5 mm thick plastic frame. Omni-Heat samples (160 μm) were cut from the inside of a Columbia brand jacket.

4.3. Environmental Chamber and Thermoregulation Characterization. An insulated chamber 12″ × 12″ × 9″ was made with R-5 insulation board. Two silicone heaters (Tempco, 5 × 5 cm^2) were inset into a block of insulation with thermistors placed atop the skin heater and between the skin and guard heater. Manila paper was chosen as the outer "skin" surface because it has an albedo representative of human skin (Figure S9). Another thermistor set 1 in. above and 1 in. to the side of the skin monitored environment temperature. This thermistor was shielded with foil to measure the true air temperature under irradiance. A cooler consisting of a pump circulating chamber air through a filled 0.5 L liquid nitrogen Dewar was used. An Adafruit Feather M0 microcontroller monitored skin temperature and adjusted the environmental temperature until T_{skin} = 33 °C using hysteresis control. The guard heater was set to maintain the same temperature within 0.3 °C as the skin heater, ensuring 1D heat transport upward. A steady-state measurement was taken such that the skin temperature varied no more than 0.3 °C over the course of at least 15 min. Error bars provided are the standard deviation of environmental temperature during the measurement. For light conditions, a Feit 33 W/300 W equivalent LED bulb was used; light intensity was measured with a light meter placed in the same position as the skin heater. The spectrum was measured with a fluorimeter (Horiba Scientific) (Figure S10). For the higher radiances (data in Figure S7), a solar simulator was used (Oriel). Measurements were taken with humidity levels in the range of 20−40%. A small thermoregulation dependence (∼1 °C) on humidity was observed (Figure S11).

4.4. Optical Characterization. A FLIR TG165 was used to measure the average infrared properties over the wavelength range 8−14 μm of the nylon, PEDOT-nylon, and AG-19. A fabric sample was placed on a heated (60 °C) 15 × 15 cm^2 copper block covered with 3M Super 88 electrical tape (ε = 0.95)[49] and the apparent emissivity (ε) was measured assuming the fabric samples (<140 μm thick) reached 60 °C. Transmissivity (τ) was measured by covering the FLIR detector with the fabric samples, measuring the apparent temperature of the 60 °C block from 6 cm away, and applying eq 1, where T_{obj} is the temperature of the fabric sample and T_{amb} is the ambient temperature.[49] Transmissivity was subtracted from apparent emissivity to obtain the true emissivity. Finally, reflectivity (ρ) was calculated from true emissivity and transmissivity by Kirchhoff's law. For our heat transfer analyses, we then assume that transmitted light is effectively absorbed (as it would be by the skin) so emissivity is reported and used assuming opaque samples. Infrared images were taken using a FLIR ONE Pro camera. The optical transmission micrograph was taken using a Nikon Ti2 Eclipse with a 40× objective and a 440 nm source.

$$\tau = \frac{T^4_{obj,apparent} - T^4_{amb}}{T^4_{obj,real} - T^4_{amb}} \quad (1)$$

4.5. Solar Radiance on a Vertical Human Body. To make the on-body radiance estimation, the human body was approximated by a vertical cylinder of height 1.7 m and surface area 1.8 m^2. Similar approximations have been previously made.[50−52] Extraterrestrial radiance values on a vertical surface on June 21st and December 21st in Boston, MA, were obtained using the SOLPOS function (NREL). On-body radiance is then approximated as 80% of extraterrestrial radiance on the projected vertical area (A_{xy} = 0.568 m^2) per total surface area (A_{tot} = 1.8 m^2) as in eq 2.

$$R_{body} = \frac{0.8 \times R_{extr} \times A_{xy}}{A_{tot}} \quad (2)$$

4.6. Wearability Characterization. The Agribon AG-19 fabric was sewn with cotton thread and ironed to form pleated baffles. The

https://doi.org/10.1021/acsami.2c23075
ACS Appl. Mater. Interfaces XXXX, XXX, XXX−XXX

PEDOT-nylon was then sewn to the bottom. During testing, the open ends of the baffles were covered with plastic and were characterized by sealing textile sample disks (3.1 cm^2) to vials containing 3 g of Dri-Rite. Placed in a sealed chamber with a humidity of ∼60%, the mass change of the vials was recorded at 2-h intervals. The mass gain was then divided by the surface area of the samples to obtain the water vapor transmission rate.

4.7. Washing Test. Textiles were washed using a 30-min total cycle. A room temperature solution of Gain laundry detergent was made per manufacturer's recommended usage and the textile was immersed with stirring for 15 min, followed by immersion in fresh DI water with stirring for 15 min. The textile was allowed to dry for at least 3 h in a hood before characterization. This procedure was repeated three times.

■ ASSOCIATED CONTENT

Supporting Information

The Supporting Information is available free of charge at https://pubs.acs.org/doi/10.1021/acsami.2c23075.

Heat transfer model assumptions and tabulated parameters used in the heat transfer model; graphical comparison to previously reported polar bear fur mimics; and additional thermoregulation and optical characterizations (PDF)

■ AUTHOR INFORMATION

Corresponding Author

Trisha L. Andrew − *Department of Chemical Engineering, University of Massachusetts Amherst, Amherst, Massachusetts 01003, United States; Department of Chemistry, University of Massachusetts Amherst, Amherst, Massachusetts 01003, United States;* orcid.org/0000-0002-8193-2912; Email: tandrew@umass.edu

Authors

Wesley Viola − *Department of Chemical Engineering, University of Massachusetts Amherst, Amherst, Massachusetts 01003, United States*

Peiyao Zhao − *Department of Chemical Engineering, University of Massachusetts Amherst, Amherst, Massachusetts 01003, United States*

Complete contact information is available at: https://pubs.acs.org/10.1021/acsami.2c23075

Author Contributions

Conceptualization: T.L.A. and W.V. Investigation: W.V. and P.Z. Writing − original draft: W.V. Writing − review and editing: W.V., T.L.A., and P.Z.

Funding

This material is based on work supported by the National Science Foundation under CBET 1706633.

Notes

The authors declare no competing financial interest.

■ ACKNOWLEDGMENTS

The authors acknowledge Alex Curtiss for assisting with the environmental chamber control system, Oscar Zabala-Ferrera for assisting with the optical transmission microscopy, and Teal M. Brechtel for assisting with manuscript edits.

■ REFERENCES

(1) Wehner, R.; Camino, F.; Shi, N. N.; Bernard, G. D.; Tsai, C.-C.; Yu, N. Keeping Cool: Enhanced Optical Reflection and Radiative Heat Dissipation in Saharan Silver Ants. *Science* **2015**, *349*, 298−301.

(2) Khattab, M. Q.; Tributsch, H. Fibre-Optical Light Scattering Technology in Polar Bear Hair: A Re-Evaluation and New Results. *J. Adv. Biotechnol. Bioeng.* **2016**, *3*, 38−51.

(3) Hegna, R. H.; Nokelainen, O.; Hegna, J. R.; Mappes, J. To Quiver or to Shiver: Increased Melanization Benefits Thermoregulation, but Reduces Warning Signal Efficacy in the Wood Tiger Moth. *Proc. R. Soc. B: Biol. Sci.* **2013**, *280*, No. 20122812.

(4) Bahners, T.; Schlosser, U.; Gutmann, R.; Schollmeyer, E. Textile Solar Light Collectors Based on Models for Polar Bear Hair. *Sol. Energy Mater. Sol. Cells* **2008**, *92*, 1661−1667.

(5) Grojean, R. E.; Sousa, J. A.; Henry, M. C. The Efficacy of Solar Conversion in a Polar Environment. *Sol. Energy* **1980**, *25*, 537−542.

(6) Øritsland, N. A.; Ronald, K. Solar Heating of Mammals: Observations of Hair Transmittance. *Int. J. Biometeorol.* **1978**, *22*, 197−201.

(7) Øritsland, N. A. Wavelength-Dependent Solar Heating of Harp Seals (Pagophilus groenlandicus). *Comp. Biochem. Physiol.* **1971**, *40A*, 359−361.

(8) Mostert, A. B. Melanin, the What, the Why and the How: An Introductory Review for Materials Scientists Interested in Flexible and Versatile Polymers. *Polymers* **2021**, *13*, No. 1670.

(9) Xiao, M.; Shawkey, M. D.; Dhinojwala, A. Bioinspired Melanin-Based Optically Active Materials. *Adv. Opt. Mater.* **2020**, *8*, No. 2000932.

(10) Berthier, S. Thermoregulation and Spectral Selectivity of the Tropical Butterfly Prepona Meander: A Remarkable Example of Temperature Auto-Regulation. *Appl. Phys. A* **2005**, *80*, 1397−1400.

(11) Walsberg, G. E. Quantifying Radiative Heat Gain in Animals. *Integr. Comp. Biol.* **1992**, *32*, 217−223.

(12) Rogalla, S.; Patil, A.; Dhinojwala, A.; Shawkey, M. D.; D'Alba, L. Enhanced Photothermal Absorption in Iridescent Feathers. *J. R. Soc. Interface* **2021**, *18*, No. 20210252.

(13) Peng, Y.; Cui, Y. Advanced Textiles for Personal Thermal Management and Energy. *Joule* **2020**, *4*, 724−742.

(14) Fang, Y.; Chen, G.; Bick, M.; Chen, J. Smart Textiles for Personalized Thermoregulation. *Chem. Soc. Rev.* **2021**, *50*, 9357−9374.

(15) Zhang, Y.; Li, Y.; Li, K.; Kwon, Y. S.; Tennakoon, T.; Wang, C.; Chan, K. C.; Fu, S. C.; Huang, B.; Chao, C. Y. H. A Large-Area Versatile Textile for Radiative Warming and Biomechanical Energy Harvesting. *Nano Energy* **2022**, *95*, No. 106996.

(16) Hsu, P. C.; Liu, X.; Liu, C.; Xie, X.; Lee, H. R.; Welch, A. J.; Zhao, T.; Cui, Y. Personal Thermal Management by Metallic Nanowire-Coated Textile. *Nano Lett.* **2015**, *15*, 365−371.

(17) Huang, J.; Li, Y.; Xu, Z.; Li, W.; Xu, B.; Meng, H.; Liu, X.; Guo, W. An Integrated Smart Heating Control System Based on Sandwich-Structural Textiles. *Nanotechnology* **2019**, *30*, No. 325203.

(18) Zhang, X. A.; Yu, S.; Xu, B.; Li, M.; Peng, Z.; Wang, Y.; Deng, S.; Wu, X.; Wu, Z.; Ouyang, M.; Wang, Y. Dynamic Gating of Infrared Radiation in a Textile. *Science* **2019**, *363*, 619−623.

(19) Engelhardt, S.; Sarsour, J. Solar Heat Harvesting and Transparent Insulation in Textile Architecture Inspired by Polar Bear Fur. *Energy Build.* **2015**, *103*, 96−106.

(20) Volesky, N.; Wagner, K.Row Covers, 2020. https://digitalcommons.usu.edu/extension_curall/2146.

(21) Jia, H.; Zhu, J.; Debeli, D. K.; Li, Z.; Guo, J. Solar Thermal Energy Harvesting Properties of Spacer Fabric Composite Used for Transparent Insulation Materials. *Sol. Energy Mater. Sol. Cells* **2018**, *174*, 140−145.

(22) Alberghini, M.; Hong, S.; Lozano, L. M.; Korolovych, V.; Huang, Y.; Signorato, F.; Zandavi, S. H.; Fucetola, C.; Uluturk, I.; Tolstorukov, M. Y.; Chen, G.; Asinari, P.; Osgood, R. M.; Fasano, M.; Boriskina, S. V. Sustainable Polyethylene Fabrics with Engineered Moisture Transport for Passive Cooling. *Nat. Sustainability* **2021**, *4*, 715−724.

(23) Guidetti, G.; Wang, Y.; Omenetto, F. G. Active Optics with Silk. *Nanophotonics* **2020**, *10*, 137−148.
(24) Viola, W.; Andrew, T. L. Sustainable Polymer Materials for Flexible Light Control and Thermal Management. *J. Polym. Sci.* **2022**, *60*, 290−297.
(25) Xu, C.; Stiubianu, G. T.; Gorodetsky, A. A. Adaptive Infrared-Reflecting Systems Inspired by Cephalopods. *Science* **2018**, *359*, 1495−1500.
(26) Zhang, L.; Fairbanks, M.; Andrew, T. L. Rugged Textile Electrodes for Wearable Devices Obtained by Vapor Coating Off-the-Shelf, Plain-Woven Fabrics. *Adv. Funct. Mater.* **2017**, *27*, No. 1700415.
(27) Lenz, A.; Kariis, H.; Pohl, A.; Persson, P.; Ojamäe, L. The Electronic Structure and Reflectivity of PEDOT:PSS from Density Functional Theory. *Chem. Phys.* **2011**, *384*, 44−51.
(28) Asplund, M.; Nyberg, T.; Inganäs, O. Electroactive Polymers for Neural Interfaces. *Polym. Chem.* **2010**, *1*, 1374−1391.
(29) Cai, L.; Song, A. Y.; Wu, P.; Hsu, P. C.; Peng, Y.; Chen, J.; Liu, C.; Catrysse, P. B.; Liu, Y.; Yang, A.; Zhou, C.; Zhou, C.; Fan, S.; Cui, Y. Warming Up Human Body by Nanoporous Metallized Polyethylene Textile. *Nat. Commun.* **2017**, *8*, No. 496.
(30) Stegmaier, T.; Linke, M.; Planck, H. Bionics in Textiles: Flexible and Translucent Thermal Insulations for Solar Thermal Applications. *Philos. Trans. R. Soc. A* **2009**, *367*, 1749−1758.
(31) Yue, X.; He, M.; Zhang, T.; Yang, D.; Qiu, F. Laminated Fibrous Membrane Inspired by Polar Bear Pelt for Outdoor Personal Radiation Management. *ACS Appl. Mater. Interfaces* **2020**, *12*, 12285−12293.
(32) Cui, Y.; Gong, H.; Wang, Y.; Li, D.; Bai, H. A Thermally Insulating Textile Inspired by Polar Bear Hair. *Adv. Mater.* **2018**, *30*, No. 1706807.
(33) Li, K.; Chang, T. H.; Li, Z.; Li, H.; Li, F. Fu.; Li, T.; Ho, J. S.; Chen, P. Y. Biomimetic MXene Textures with Enhanced Light-to-Heat Conversion for Solar Steam Generation and Wearable Thermal Management. *Adv. Energy Mater.* **2019**, *9*, No. 1970141.
(34) August, A.; Kneer, A.; Reiter, A.; Wirtz, M.; Sarsour, J.; Stegmaier, T.; Barbe, S.; Gresser, G. T.; Nestler, B. A Bionic Approach for Heat Generation and Latent Heat Storage Inspired by the Polar Bear. *Energy* **2019**, *168*, 1017−1030.
(35) Du, A.; Wang, H.; Zhou, B.; Zhang, C.; Wu, X.; Ge, Y.; Niu, T.; Ji, X.; Zhang, T.; Zhang, Z.; Wu, G.; Shen, J. Multifunctional Silica Nanotube Aerogels Inspired by Polar Bear Hair for Light Management and Thermal Insulation. *Chem. Mater.* **2018**, *30*, 6849−6857.
(36) Chang, Y.; Lee, K.; Kiebooms, R.; Aleshin, A.; Heeger, A. J. Reflectance of Conducting Poly(3,4-ethylenedioxythiophene). *Synth. Met.* **1999**, *105*, 203−206.
(37) Tong, J. K.; Huang, X.; Boriskina, S. V.; Loomis, J.; Xu, Y.; Chen, G. Infrared-Transparent Visible-Opaque Fabrics for Wearable Personal Thermal Management. *ACS Photonics* **2015**, *2*, 769−778.
(38) Olesen, B. W.; Moreno-Beltron, D. L.; Grau-Rios, M.; Tahti, E.; Niemela, R.; Olander, L.; Hagstrom, K.Target Levels. In *Industrial Ventilation Design Guidebook*; Elsevier B.V., 2001; pp 355−413.
(39) Bass, M. *Handbook of Optics*; McGraw-Hill, 2010.
(40) Blazejczyk, K.; Nilsson, H.; Holmér, I. Solar Heat Load on Man - Review of Different Methods of Estimation. *Int. J. Biometeorol.* **1993**, *37*, 125−132.
(41) Strobach, E. M.; Boriskina, S. V. Daylighting. *Opt. Photonics News* **2018**, *29*, 25−31.
(42) National Fire Protection Association. *NFPA 70: National Electrical Code 2020*, 2020.
(43) Chen, S.; Kang, E. S. H.; Shiran Chaharsoughi, M.; Stanishev, V.; Kühne, P.; Sun, H.; Wang, C.; Fahlman, M.; Fabiano, S.; Darakchieva, V.; Jonsson, M. P. Conductive Polymer Nanoantennas for Dynamic Organic Plasmonics. *Nat. Nanotechnol.* **2020**, *15*, 35−40.
(44) Barnes, W. L.; Dereux, A.; Ebbesen, T. W. Surface Plasmon Subwavelength Optics. *Nature* **2003**, *424*, 824−830.
(45) Ebbesen, T. W.; Lezec, H. J.; Ghaemi, H. F.; Thio, T.; Wolff, P. A. Extraordinary Optical Transmission through Sub-Wavelength Hole Arrays. *Nature* **1998**, *391*, 667−669.
(46) Karst, J.; Floess, M.; Ubl, M.; Dingler, C.; Malacrida, C.; Steinle, T.; Ludwigs, S.; Hentschel, M.; Giessen, H. Electrically Switchable Metallic Polymer Nanoantennas. *Science* **2021**, *374*, 612−616.
(47) Howden, R. M.; Flores, E. J.; Bulović, V.; Gleason, K. K. The Application of Oxidative Chemical Vapor Deposited (oCVD) PEDOT to Textured and Non-Planar Photovoltaic Device Geometries for Enhanced Light Trapping. *Org. Electron.* **2013**, *14*, 2257−2268.
(48) Kuznetsov, A. I.; Miroshnichenko, A. E.; Brongersma, M. L.; Kivshar, Y. S.; Luk'yanchuk, B. Optically Resonant Dielectric Nanostructures. *Science* **2016**, *354*, No. eaag2472.
(49) Madding, R. P.In *Emissivity Measurement and Temperature Correction Accuracy Considerations*, Thermosense XXI, 1999; pp 393−401.
(50) Underwood, C. R.; Ward, E. J. The Solar Radiation Area of Man. *Ergonomics* **1966**, *9*, 155−968.
(51) Vanos, J. K.; Rykaczewski, K.; Middel, A.; Vecellio, D. J.; Brown, R. D.; Gillespie, T. J. Improved Methods for Estimating Mean Radiant Temperature in Hot and Sunny Outdoor Settings. *Int. J. Biometeorol.* **2021**, *65*, 967−983.
(52) Kenny, N. A.; Warland, J. S.; Brown, R. D.; Gillespie, T. G. Estimating the Radiation Absorbed by a Human. *Int. J. Biometeorol.* **2008**, *52*, 491−503.

NOTE ADDED IN PROOF

"sun" by Matias Canobra is licensed under CC BY 3.0. "Six-Spotter Forester" by Brooke Lewis is licensed under CC BY 3.0. "polar bear" by Tamiko Young is licensed under CC BY 3.0.

https://doi.org/10.1021/acsami.2c23075
ACS Appl. Mater. Interfaces XXXX, XXX, XXX−XXX